HHS Public Access

Author manuscript

Clin Exp Metastasis. Author manuscript; available in PMC 2016 April 13.

Published in final edited form as:

Clin Exp Metastasis. 2010 April ; 27(4): 217–231. doi:10.1007/s10585-010-9320-5.

Targeting activated integrin αvβ3 with patient-derived antibodies impacts late-stage multiorgan metastasis

Karin Staflin[1], **Joseph S Krueger**[1], **Janna Hachmann**[1], **Jane S Forsyth**[1], **Mihaela Lorger**[1], **Sebastian CJ Steiniger**[2], **Jenny Mee**[2], **Cristina Pop**[3], **Guy S Salvesen**[3], **Kim D Janda**[2], and **Brunhilde Felding-Habermann**[1]

[1]Department of Experimental Medicine, The Scripps Research Institute, La Jolla, CA 92037, USA

[2] Department of Chemistry, The Scripps Research Institute, La Jolla, CA 92037, USA

[3] Program in Cell Death and Apoptosis Research, The Burnham Institute, La Jolla, CA 92037, USA

Abstract

Advanced metastatic disease is difficult to manage and specific therapeutic targets are rare. We showed earlier that metastatic breast cancer cells use the activated conformer of adhesion receptor integrin αvβ3 for dissemination. We now investigated if targeting this form of the receptor can impact advanced metastatic disease, and we analyzed the mechanisms involved. Treatment of advanced multi-organ metastasis in SCID mice with patient-derived scFv antibodies specific for activated integrin αvβ3 caused stagnation and regression of metastatic growth. The antibodies specifically localized to tumor lesions *in vivo* and inhibited αvβ3 ligand binding at nanomolar levels *in vitro*. At the cellular level, the scFs associated rapidly with high affinity αvβ3 and dissociated extremely slowly. Thus, the scFvs occupy the receptor on metastatic tumor cells for prolonged periods of time, allowing for inhibition of established cell interaction with natural αvβ3 ligands. Potential apoptosis inducing effects of the antibodies through interaction with caspase-3 were studied as potential additional mechanism of treatment response. However, in contrast to a previous concept, neither the RGD-containing ligand mimetic scFvs nor RGD peptides bound or activated caspase-3 at the cellular or molecular level. This indicates that the treatment effects seen in the animal model are primarily due to antibody interference with αvβ3 ligation. Inhibition of advanced metastatic disease by treatment with cancer patient derived single chain antibodies against the activated conformer of integrin αvβ3 identifies this form of the receptor as a suitable target for therapy.

Keywords

advanced metastasis; treatment; activated integrin; patient antibodies

Correspondence: B. Felding-Habermann, The Scripps Research Institute, MEM 150, 10550 North Torrey Pines Road, La Jolla, CA 92037, brunie@scripps.edu.

All animal work was performed in accordance with NIH guidelines and approved by the Institutional Animal Care and Use Committee of The Scripps Research Institute Animal Resources (AAALAC accredited)

INTRODUCTION

Advanced multi-organ metastasis is difficult to manage, and therapies could be improved if new functional targets on tumor cells were identified (1). A potential target for inhibition of metastatic growth is the high affinity conformer of adhesion receptor integrin αvβ3. αvβ3 is an important player in tumor angiogenesis, but it also promotes tumor cell adhesion, invasive migration and survival (2-6). The expression of αvβ3 in tumors and the tumor associated vasculature correlates with tumor grade and progression in several tumor types, most prominently in melanoma, glioma, and breast cancer (4;7-10). αvβ3 antagonists, including antibodies, can disrupt tumor-induced angiogenesis in animal models (11-13) and interfere with metastasis promoting tumor cell functions (14-16). We previously documented that the activation state of αvβ3 is critical for supporting metastatic progression and that the high affinity form of αvβ3 identifies a metastatic subset of tumor cells (5). Interestingly, we also found that the immune repertoire of cancer patients can contain anti-tumor antibodies, which specifically react with the activated form of αvβ3. These antibodies are ligand-mimetics of the αvβ3 integrin and carry an Arg-Gly-Asp (RGD) sequence within their CDR-H3 regions (17).

In the present study, we investigated whether targeting the high affinity conformer of integrin αvβ3 with the ligand mimetic antibodies can interfere with advanced metastatic disease. This was examined in immune deficient mice after inducing progressive metastatic burden with human tumor cells expressing high affinity αvβ3. Response to treatment was followed with non-invasive bioluminescence imaging. The observed anti-metastatic properties of the scFv antibodies are due to their ability to specifically and nearly irreversibly bind and inhibit the activated conformer of αvβ3. Thus, activated αvβ3 appears as a suitable target for the inhibition of widespread metastatic disease. The fully human antibodies used in this study and their derivatives, or compounds with similar specific properties, might provide a basis for powerful therapeutic intervention of advanced metastasis.

RESULTS

The main goal of this study was to investigate if the high affinity conformer of tumor cell integrin αvβ3 is a suitable target for inhibition of advanced and widespread metastatic disease. We used human tumor cell models expressing activated αvβ3 in immune deficient mice, and analyzed the ability of patient derived scFv antibodies against this form of the receptor to interfere with advanced metastatic progression.

Antibody binding validation and routes of administration

To test in principle whether targeting activated αvβ3 with the ligand mimetic scFvs interfere with advanced metastatic disease, we chose a phage-displayed format of the antibodies for treatment. By using this format, we took advantage of the tissue penetrating properties of phage and their ability for multivalent antibody display (18). To verify the cell binding characteristics of the phage antibodies, we analyzed each scFv-phage batch for tumor cell binding before using the material for animal treatment. ScFv phage binding was examined on two different tumor cell models, each expressing the activated form of integrin αvβ3,

namely M21 human melanoma cells (high αvβ3 expression) and MDA-MB-435 $\beta3_{D723R}$ human metastatic cancer cells (5) (intermediate αvβ3 expression). Binding of αvβ3 directed scFv1- and scFv5-phage was compared to wild type phage as a control (Fig. 1A). Appropriate routes of administration and *in vivo* distribution of scFv phage were examined in non-tumor bearing mice to assess if and to what extent the antibodies were able to reach major target organs of metastasis, without the bias of tumor burden there. Inoculation of 5×10^{10} scFv1 or scFv5 phage intranasally, intravenously or intraperitoneally lead to efficient phage recovery from the lungs, brain, liver, and kidneys of SCID mice 24 hours after scFv injection (Fig. 1B shows scFv5). Intravenous and intraperitoneal routes produced the highest phage titers in the examined organs ($>1\times10^8$ phages per gram of tissue). The lowest titer was found in the brain. Having established that scFv phage can reach sites that are most frequently involved in metastasis, we chose the intraperitoneal route for scFv phage treatment of tumor bearing animals, as this route lead to high phage tissue recovery and can be used repeatedly for treatment.

Treatment of metastatic disease with scFv antibodies targeting activated integrin αvβ3

Metastasis was induced in SCID mice by injecting MDA-MB-435 human metastatic cancer cells (19;20) into the venous circulation. The tumor cells were stably tagged with Firefly luciferase to follow their growth and response to treatment based on non-invasive longitudinal measurements by bioluminescence signal of whole body imaging. For the treatment studies, scFv phage purification was optimized to remove endotoxin, and it was verified that phage injection had no adverse side effects. Metastatic burden was monitored in each animal over time and measured based on photon flux ($p/s/cm^2$). The fold-change in lesion growth under treatment was calculated by comparing lesion growth during a given number of days before treatment and the same number of days under treatment.

An overview of treatment responsiveness in animals with advanced metastatic burden and response types is given in Table 1. The results indicate that scFv1 or scFv5 treatment interfered with *in vivo* growth of metastatic lesions in a significant number of animals compared to treatment controls ($p=0.0164$ by Fisher exact test).

Treatment response measurements initially focused on lung lesions because these represented the strongest burden and were consistently found. Figure 2 shows mice where metastatic lesions were allowed to develop for 56 days before starting i.p. treatment with scFv1 or scFv 5 phage (5×10^{10}). The animals in panels A-C had received 1×10^5 tumor cells and were treated every 48 hrs for seven days (4 doses). The percentage of responding animals was 57% in the scFv1 group, and 60% in the scFv5 group. To challenge the therapeutic approach and assess treatment responses in mice with even stronger metastatic burden, mice as shown in panel D were injected with 2.5×10^5 tumor cells and received treatment on day 56 given every 24 h (8 doses). Under these conditions, the response rate was 75% in the scFv1 group, and 25% in the scFv5 group. All control animals showed continuous lesion progression. Treatment efficacy of scFv1 was higher than that of scFv5. This finding corresponds to an enhanced potency of scFv1 for interfering with αvβ3 integrin ligand binding, as shown below. The results indicate that targeting the high affinity form of integrin αvβ3 can impact advanced metastatic burden and slow its growth.

To emulate a clinical situation where patients may present with widespread advanced metastatic disease to multiple organs, and to monitor treatment response of lesions at individual target sites, we injected SCID mice i.v. with a subline of MDA-MD 435 (MDA-MB 435 met) that we selected *in vivo*. This subline expresses intrinsically activated integrin αvβ3, and consistently causes multiorgan metastasis. All injected mice developed metastatic lesions in multiple target organs, including the brain, lymph nodes, liver, spleen, bone, kidneys and lungs. We selected the animals with the highest tumor burden and the most widespread metastasis for therapy with scFv1 or scFv 5 phage. Individual animals had metastases in up to three different organs. In all cases, these included the lung. The animals were treated every 24h for 7 days with 5×10^{10} scFv1 or scFv5 phage, and lesion growth was monitored by bioluminescence imaging. The results are summarized in Table 2, reporting regression of pulmonary and extrapulmonary metastases in the treatment groups. Examples of regression in renal metastases in response to only three doses of scFv1 treatment are shown in Fig. 3. In one case, an adrenal lesion, clearly documented before treatment, disappeared and was no longer detectable by non-invasive whole body imaging (Fig. 3B Mouse 1) or by *ex vivo* imaging of the excised organ. In another case, a large adrenal lesion clearly regressed in response to scFv1 (Fig. 3B Mouse 2).

Metastatic lesions in different organs within the same animal sometimes showed distinct responses to treatment. There was no apparent correlation between lesion size at the beginning of treatment and the ability to respond. Differences in the vascularity of the lesions and vascular functionality, as well as heterogeneity of individual lesions might contribute to this observation. Overall, scFv1 treatment induced regression in multi-organ metastasis more efficiently than scFv5. All animals treated with control phage showed continuous progression in individual lesions and overall tumor burden.

In vivo localization of scFv to metastatic lesions and in situ treatment response

Having evidence that scFv1 or scFv 5 treatment directed against the high affinity conformer of integrin αvβ3 can interfere with advanced metastatic growth, we investigated whether the antibodies actually reached the tumor cells within metastatic lesions to assess whether the tumor cells are direct targets of this treatment. To track the antibodies in lesion bearing animals that had received scFv1 or scFv5, the animals were terminally perfused 24 hours after the last antibody dose and cryosections prepared of control and tumor bearing organs. Tumor cells were identified by staining for human CD44 (21) (dark blue in Fig. 4A), and scFv phage was detected with anti-M13 (brown in Fig. 4A or red fluorescence in 4B). As indicated in Figure 4A, showing phage signal within metastatic lesion tissue particularly at higher magnification (right panel), and clearly seen by imunofluorescence staining in Figure 4B, ScFv1 and scFv 5 phage specifically accumulated within metastatic lesions and in their immediate proximity. This was observed in different organs with metastatic burden, but not in non-tumor bearing tissues. Wild type phage, used as a control, did not accumulate at tumor lesions. Non-tumor bearing tissues sporadically showed a faint signal for wild type phage, but not associated with any specific cell type. Figure 4 documents that scFv1 and scFv5 phage localized to lung or lymph node metastases. In some cases, scFv signal was found directly associated with the tumor cells. An example of a lung lesion is shown by deconvolution microscopy in Fig. 4B (bottom row). These results indicate that the ligand

mimetic antibodies, directed against the activated conformer of integrin αvβ3, localized to advanced metastatic lesions in the mouse model in a therapeutic setting. Integrin αvβ3 is known to be a key player in angiogenesis, and the activated form of the receptor is expressed by sprouting endothelial cells (22). We found that the patient derived antibodies, scFv1 and scFv5, react with the murine antigen (by flow cytometry on proliferating murine endothelial cells and the Bend3 endothelial cell line, not shown). However, there was no difference in micro vessel density within lung tumor lesions in control versus antibody treated animals. This was measured on anti- CD34 stained step sections covering 600-800 μm depth of lung tissue (data not shown). There was a tendency for fewer lesions in the lungs of animals responding to treatment (1-9 lesions) compared to controls (10-25 lesions).

To investigate how scFv treatment targeting the activated conformer of integrin αvβ3 affects lesion development *in vivo*, we studied cell cycle marker expression in lung metastases that responded to scFv treatment. Compared to controls, the number of proliferating Ki67-positive cells was significantly reduced in lesions responding to treatment (Fig. 5A). Expressed as percent area covered by Ki67 signal of total lesion area measured, the mean Ki67 reactivity in control and non-responding lesions was 38.1 ± 6.9%, and 19.9 ± 7.4% in responding lesions ($p=0.0159$). In addition, the responding lesions showed enhanced infiltration by activated macrophages (F4/80 signal) (Fig. 5B). The results indicate that scFv treatment affected the growth rate of metastatic lesions at the cellular level and involved host cell responses. These responses potentially helped to clear apoptotic or dead tumor cells, which were rarely detected (not shown).

Inhibition of receptor-ligand binding at the molecular level

To investigate mechanisms involved in the observed treatment responses, we studied the interactions of the ligand-mimetic antibodies and integrin αvβ3 at the molecular and cellular levels.

To assess molecular interactions between integrin αvβ3 and the scFv antibodies, we analyzed their ability to interfere with ligand binding to the purified receptor. Vitronectin, fibronectin and fibrinogen are natural ligands of αvβ3 in extracellular matrices and plasma. A hallmark characteristic of the activated conformer of αvβ3 is that the receptor can recognize these ligands as soluble proteins. Incubation of the biotinylated proteins with immobilized αvβ3 in the presence of cations and increasing concentrations of the antibodies showed that scFv 1 and scFv 5 efficiently interfered with αvβ3 ligand binding (Fig. 6A). The half maximal inhibitory concentrations (IC_{50}) for scFv 1 were 1.25 nM for vitronectin, 0.71 nM for fibronectin, and 0.35 nM for fibrinogen. For scFv 5, the IC_{50} values were 25 nM for vitronectin, 12.5 nM for fibronectin, and 10.7 nM for fibrinogen. ScFv20 used as a control antibody failed to inhibit. While patient derived scFv antibodies scFv 1 and scFv 5 contain the RGD integrin binding motif within their CDR-H3 regions and are specific for αvβ3, scFv 20 lacks the RGD motif, does not block function and detects αv integrins regardless of their β subunit association (17). The results demonstrate that scFv1 and scFv 5 have a high affinity for αvβ3 and compete very effectively with ligands binding to this receptor. The increased inhibitory efficacy of scFv1 over scFv5 at the molecular level is reflected in the increased anti-cancer efficacy of scFv1 seen *in vivo*.

Characteristics of scFv binding to human tumor cells expressing activated integrin αvβ3

To understand inhibitory activities of scFv1 and scFv5 on tumor cell functions that rely on integrin αvβ3 and might promote metastasis, we analyzed interaction between the scFvs and tumor cell expressed αvβ3. Integrin binding of natural ligands in their soluble form requires the high affinity state of the receptor (23). Furthermore, tumor cells within target tissues interact dynamically with components of the extracellular matrix and derive signals from their matrix environment for survival and growth. To investigate the binding characteristics of tumor cell expressed high affinity αvβ3 and the ligand mimetic scFvs, we analyzed cellular association and dissociation. All scFv cell binding experiments were carried out at 0°C to prevent internalization. Flow cytometry binding analysis of fluorescinated scFv5 protein and MDA-MB 435 human metastatic cancer cells, expressing either activated high-affinity $\alpha v\beta 3_{D723R}$ or non-activated $\alpha v\beta 3_{WT}$, indicated that the ligand-mimetic antibody depended on αvβ3 activation for efficient binding. Binding was experimentally maximized in the presence of Mn^{2+} (Fig. 6B, left panel), a cation known to induce a high affinity state in integrin heterodimers (24-26). Using a Mn^{2+} concentration (25 μM) that supports suboptimal (75%) scFv5 binding to tumor cells expressing the intrinsically activated receptor ($\beta 3_{D723R}$ mutant), we titrated the antibody to determine binding saturation. Saturable binding in the presence of divalent cations indicated specificity and cation dependence (Fig. 6B, right panel). These findings underscore the ligand mimetic nature of the scFv antibodies and define conditions suitable to determine cellular association and dissociation of the antibodies. The association and dissociation characteristics are important for understanding the therapeutic potential of the antibodies and their ability to interfere with established αvβ3 ligand interactions. Such interactions support tumor cell integration and growth within target tissues of metastasis.

Using tumor cells expressing intrinsically activated $\alpha v\beta 3_{D723R}$ and 25μM Mn^{2+}, we found that the ligand mimetic antibodies scFv1 and scFv5 exhibit a fast cellular association rate, with half maximal binding observed after 5 min, the earliest measured time point (shown for scFv 5 in Fig. 6C, left panel). In contrast, scFv dissociation after binding saturation was exceedingly slow, with only 22% binding loss after 160 min, whereas binding of fibrinogen, a natural ligand of αvβ3, was reduced by 50% after 60 min, and 88% after 120 min (Fig. 6C, right panel). These results indicate that the ligand mimetic antibodies can occupy the receptor efficiently and stay bound for prolonged periods of time. Thereby the antibodies may displace natural ligands that dissociate off the receptor. Based on these properties, the antibodies efficiently interfere with dynamic αvβ3 mediated cell adhesive functions during cell migration and invasion as previously seen *in vitro* (17). Importantly, the observed scFv cell binding characteristics likely enable the antibodies to interfere with tumor cell behavior *in vivo* and to disrupt established tumor cell adhesion mediated by integrin αvβ3.

Analysis of caspase-3 activation by the RGD-containing scFv antibodies

The *in vivo* responses to treatment with the αvβ3 ligand-mimetic scFv antibodies may have diverse underlying reasons. The antibodies could exert their therapeutic effects primarily through their ligand-mimetic nature interfering with αvβ3 ligand binding. However, additional mechanisms may also be involved. We previously showed that scFv 1 and scFv 5 are internalized by tumor cells expressing activated integrin αvβ3 and induce apoptosis (17).

We therefore reasoned that the internalized RGD-containing scFvs might interact with intracellular proteins, such as the apoptosis inducing caspase-3. Caspase-3 contains a putative RGD binding site, close to its Asp^{175} cleavage site (Asp-Asp-Met, DDM) (27;28). A previously reported intriguing concept suggested that cell internalized RGD peptides might induce apoptosis by directly binding and activating caspase-3 (27;29;30). To explore if such a mechanism might be involved in the observed anti-metastatic properties of the RGD containing scFv antibodies, we verified that the tumor cells used in our treatment study expressed caspase-3, and analyzed if the scFvs could directly interact with caspase-3 and activate the enzyme.

We confirmed caspase-3 expression in MDA-MB-435 human tumor cells used in our *in vivo* treatment study express (Fig. 7A). MCF7 cells lacking caspase-3 (31) were used as negative control, and SKBr3 (32) as positive control. To investigate if RGD containing scFv 1 and scFv 5 can directly bind caspase-3, we analyzed whether the scFvs immuno-precipitate caspase-3 from tumor cell lysates, or if the scFvs - added to tumor cell lysates - could be co-immunoprecipitated with anti-caspase-3. We found no evidence of scFvs caspase-3 interaction (not shown). Furthermore, we found no interaction between recombinant caspase-3 and RGD-containing scFv1 or scFv5 by ELISA under various cation conditions known to affect RGD binding (Fig. 7B).

Once internalized by cells, RGD-containing proteins might transiently interact with caspase-3 in a biologically relevant but difficult to detect manner. Considering the therapeutic effects on metastatic growth by the RGD-containing scFvs in our animal model, we therefore investigated whether the scFvs could contribute to caspase-3 activation in cell lysates and by using recombinant human caspase-3 protein. Hypotonic lysates of 293A cells, deprived of mitochondria and containing caspase-3, were readily activated by addition of cytochrome c and dATP to form apoptosomes that can activate caspase-3 (Fig. 7C,D). Cofactors in these gently generated lysates promote the stability of procaspase-3 and support its activation. In contrast, RGD-containing scFv 5, or RGD peptides, showed no induction of caspase-3 activity over RGE-containing scFv Mut5, or RAD, as negative controls. Similar results were obtained despite increasing scFv concentrations, and after investigating the kinetics of caspase-3 activation by continuous measurement of substrate cleavage over time (Fig. 7D). Likewise, reducing the complexity of the assay system further and using recombinant caspase-3 to ensure that the reaction and potential interaction between caspase-3 and scFv antibody was not influenced by components present in cells or cell lysates, did not reveal RGD induced caspase-3 activation (Fig.7D right). Thus, these results make it very unlikely that the internalized RGD-containing antibodies scFv1 or scFv5 induce apoptosis by direct activation of caspase-3. We therefore conclude that the inhibitory properties and *in vivo* treatment effects, that the antibodies exerted on tumor cells expressing the activated conformer of integrin $\alpha v\beta 3$ and their metastatic lesions, are most likely based on the ability of the antibodies to interfere efficiently with ligand binding to the target integrin.

DISCUSSION

Metastatic disease is mainly treated with chemotherapy to halt tumor growth or with specific inhibitors of receptors and pathways to interfere with tumor cell viability. Development of effective combinations of such therapies and discovery of new targets are urgently needed to improve therapeutic responses.

Our study explored the high affinity, activated conformer of integrin αvβ3 on metastatic tumor cells as a functional target for therapy with human antibodies that specifically recognize and block this form of the receptor. We showed earlier that a metastatic subset of human tumor cells expresses the activated integrin and uses this form of the receptor for successful early steps of dissemination to distant organs (5). Interestingly, the immune repertoire of cancer patients contains antibodies that recognize the high affinity form of αvβ3. These antibodies mimic natural ligands of the receptor through expression of an RGD integrin-binding motif within CDR-H3 of the antigen recognition site. This feature is combined with specificity for αvβ3 (17).

Integrin αvβ3 is expressed by certain invasive tumor types, such as metastatic melanoma, glioma, and breast cancer (7-10;13). The receptor is also present on angiogenic blood vessels (3) and serves as an important mediator to secure blood supply for tumor growth. As on metastatic tumor cells, αvβ3 is activated on angiogenic blood vessels (33) and potentially fulfills similar growth promoting and invasive functions of the sprouting endothelial cells. Integrin αvβ3 antagonists, targeting the receptor regardless of its functional activation state, have been used in animal models and recently in cancer patients, to curb angiogenesis and slow tumor growth (34). In the clinic, antibodies against αvβ3 and a cyclic peptide-based inhibitor of αvβ3 and αvβ5 have shown promising effects (14). MEDI-522, a second generation humanized anti-αvβ3 mAb showed low toxicity and induced stable disease in some patients with renal metastasis (35).

Generally, integrin ligation supports signal transduction that promotes cell survival, migration and proliferation (36). Transient expression of the high affinity form of certain integrins in normal cells is tightly regulated and necessary for specific functions. These include leukocyte and platelet interaction with the vessel wall during immune reactions and hemostasis (37). Expression of activated αvβ3 and the constitutive presence of the high affinity receptor on disseminating tumor cells may be key for metastatic progression. Thus, therapeutic targeting of the high-affinity conformer of αvβ3 could offer a focused strategy for interfering with metastatic growth and angiogenic support.

Here, we show that treatment of experimental mice with advanced metastatic disease induced by human tumor cells expressing activated αvβ3, can stabilize lesion growth and block progression. We applied scFv fragments of patient derived antibodies against the high affinity form of αvβ3 displayed on phage. This approach increases scFv valency and *in vivo* half-life. It also takes advantage of the phage tissue penetration properties. In the clinic, this format may not be not preferred but could be replaced with multivalent scFvs, Fab fragments or whole IgG, possibly coupled to toxins or effector molecules (38). The scFv format could be helpful for diagnosis and tumor cell tracing to report metastatic disease because of the

low molecular weight of the scFvs (27 kDa) and their rapid clearance from the circulation and tissues (18;39). To gain proof-of-principle information on whether targeting the high affinity conformer of tumor cell integrin αvβ3 can inhibit advanced and widespread metastatic disease, we increased the challenge for the therapeutic potential of the αvβ3 directed antibodies and accounted for a spectrum of clinically relevant situations. These included increased tumor burden at the beginning of treatment and the involvement of multiple and differently affected metastatic sites. The observed clinical responses indicated heterogeneity in the metastatic burden in individual animals and different target organs. This situation is clinically relevant and reflects a major challenge for new therapeutic approaches. We demonstrated that scFv antibdody phage can reach metastatic lesions. However, it is possible that not all lesions uniformly absorb the antibody and that some are not efficiently reached by the treatment due, at least in part, to irregularities in the functionality of lesion supporting blood vessels.

Generally, we found that scFv1 is a more potent inhibitor than scFv5. This was seen in the animal studies, particularly under clinically more challenging conditions, but also at the molecular level. Characterizing mechanisms involved in the observed therapeutic response of advanced metastasis to treatment with scFvs against high affinity integrin αvβ3, we found that the antibodies specifically localize to metastatic lesions and inhibit αvβ3 ligand binding in the nanomolar range. ScFv 1 is a particularly potent inhibitor and interferes with vitronectin binding 20 fold more effectively, fibronectin binding 17.6 fold more effectively, and fibrinogen binding 30.6 fold more effectively than scFv5. Both scFvs associate rapidly with αvβ3 on tumor cells and, in contrast to natural ligand, dissociate extremely slowly. This finding supports the concept that the scFvs may displace natural ligand from the receptor and block the integrin efficiently. This is relevant during adhesion and migration when αvβ3 temporarily dissociates from its natural ligands. Through this mechanism, the scFvs likely exert long-term inhibitory functions and may effectively impact tumor cell survival and growth mediated by high affinity αvβ3. In addition to inhibiting activated αvβ3 on tumor cells, the scFvs might interfere with tumor angiogenesis. We found that the ligand mimetic scFvs react with the murine receptor. However, we did not see differences in microvessel density in lesions of control versus antibody treated animals.

It is well known that RGD-containing peptides can induce apoptosis by binding to integrins and blocking their functions. Several intriguing reports suggested an additional mechanism through which RGD-containing molecules might impact tumor cell survival (27;29;30). Upon cell internalization, RGD peptides were proposed to interact with an RGD-binding site within procaspase-3 (27;28). It was claimed that interactions between the RGD-binding site and RGD-peptides could induce auto-activation of caspase-3. This concept had garnered high attention in the integrin field as it indicated that RGD containing compounds might interfere with tumor cell viability not by inhibiting integrin mediated adhesion, but directly by triggering an apoptotic response through activation of caspase-3, using integrins merely as docking molecules for cell internalization. In fact, we showed earlier that tumor cells expressing activated αvβ3 can internalize the ligand mimetic scFvs used in this study, and respond with apoptosis (17). Because of the clinical relevance of our finding that the RGD containing patient derived antibodies could interfere with late stage metastasis, we systematically investigated the ability of the RGD containing scFvs and RGD peptides to

bind and directly activate tumor cell caspase-3. However, we did not detect any interaction between caspase-3 and the scFvs or RGD-peptides. In addition, we found no evidence for procaspase-3 activation in cell lysates or using recombinant caspase protein. Therefore, the therapeutic effects of the RGD containing antibody fragments are most likely due to their high affinity to αvβ3 and potent and persistent ability to interfere with αvβ3 ligation.

Together, our results indicate that the high affinity conformer of integrin αvβ3, expressed by a metastatic subset of human tumor cells, is a promising target for inhibition of advanced and widespread metastatic disease. The activated receptor can be efficiently blocked with antibodies from the cancer patient immune repertoire, which interfere with metastatic growth.

MATERIALS AND METHODS

scFv protein and phage production and preparation for *in vivo* use

ScFv antibodies directed against activated integrin αvβ3, svFv1 and scFv 5, (17) were displayed as pIII fusion proteins on M13 bacteriophage and expressed in E. coli. Phage or scFv protein were purified as described (40). For *in vivo* use, endotoxin was removed from phage preparations by repeated phase separations using 1% Triton X-114 (41). Phage was further purified on protein purification spin columns (Pierce, Rockford IL) and sterile filtered. Phage titer was determined by infecting *E.coli* TG1 with serial dilutions (1×10^4 - 1×10^{10} fold) and enumerating colonies on carbenicillin containing agar plates. Phage titers were generally around 10^{11}/ml.

In vivo Phage distribution

Phage were injected i.v, i.p or applied intranasally into non-tumor bearing mice to determine phage organ distribution. For intranasal gavage, a phage volume of 10μl was administered directly into the nostrils in 2 μl increments over 5 min. The organs were harvested and weighed 24h after phage injection, homogenized in PBS, washed and serially diluted to infect bacteria before counting carbenicillin resistant colonies to calculate the number of phages per gram of tissue.

Analysis of scFv cell binding by flow cytometry

Before use in animals, each scFv phage batch was analyzed by flow cytometry for binding to tumor cells expressing high affinity integrin αvβ3 in the presence of Ca^{2+} (17). Phage-ScFvs were used at a concentration of 5×10^8 in TBS and incubated with cells on ice, followed by murine anti-M13 mAb 10μg/ml (Exalpha Biologicals, Watertown, MA) and goat FITC-anti mouse 1:50 (Zymed, San Francisco, CA).

In vivo treatment of metastatic disease

Advanced metastatic burden for analysis of treatment response was induced by tail vein injection of 6-8 week old CB.17 SCID mice with 1×10^5 – 2.5×10^5 luciferase tagged MDA-MB 435 or MDA-MB 435-met cells (*in vivo* selected for enhanced metastatic activity). scFv phage were prepared freshly for each experiment and binding activity validated. Mice were assigned to experimental groups based on noninvasive imaging (photon flux as p/s/cm^2)

(IVIS 200, Caliper Lifesciences, Alameda, CA) so that control and scFv treatment groups included animals with a similar range of metastatic burden. Under treatment, location and extent of lesion growth were again monitored by bioluminescence imaging, followed by histology.

Deeply anesthetized mice were terminally perfused through the ascending aorta with saline followed by 4% paraformaldehyde (PFA). The perfused organs were post-fixed in para formaldehyde for 4h before transfer into 25% sucrose in phosphate buffer. Frozen tissues were cryo sectioned (35 μm) and stored in cryoprotective solution at −20°C. For analyses of phage tissue distribution and phage titer, animals were euthanized 24h after the last phage injection (i.v., i.p., or intranasal) and organs were weighed and homogenized, followed by infection of bacteria with the extracts. The numbers of carbenicillin resistant colonies (bacteria infected with phage) were counted, and phage count was normalized to phages per gram of tissue. All animal work was performed in accordance with The Scripps Research Institute Animal Resources (AAALAC accredited).

Definition of treatment response and statistical analysis

Late stages of metastatic growth present a high level of complexity and variations in the extent and distribution of metastatic burden from experimental animal to animal. Therefore, we chose analysis criteria similar to “Response Evaluation Criteria in Solid Tumors” (42-44). These criteria are used in clinical trials for treatment of advanced metastatic disease to assess individual treatment responses. Treatment responses were evaluated based on longitudinal measurements of tumor cell signal by noninvasive bioluminescence imaging of metastatic burden, before and during treatment in each animal. If, in a given experiment, an animal was treated for 7 days, then lesion growth during the 7-day period before treatment was compared to lesion growth during the 7 days of treatment. The difference in tumor growth before and during treatment was calculated. The resulting fold-changes were defined as: Progression (>1.3 fold), Stabilization (0.7-1.3 fold), Reduced Progression (0.1-0.7 fold), or Regression (<0.1 fold). It was then determined how the animals in each group distributed between the response categories. For comparison of responses between the three treatment groups, scFv1, scFv5, and wild type phage as control, we note that the overall likelihood ratio chi-squared statistic with 6 degrees of freedom may be partitioned into two independent components, each with 3 degrees of freedom: the first component corresponds to comparison of ScFv1 vs. ScFv5, and the second component corresponds to the comparison of controls to the pooled ScFv1/ScFv5 category (45). We report Fisher exact tests for these component comparisons.

Immunohistochemistry

To detect scFv phage in tumor lesions, free floating tissue sections were quenched with 3% H_2O_2 (in case of DAB staining) and blocked with goat serum for 1h, before adding a primary antibody against human CD44 (Mab 29.7 at 1:50 dilution of hybridoma supernatant) kindly provided by Jim Quigley, TSRI (21), or M13 phage (anti-M13, Exalpha Biologicals Inc. Watertown, MA, at 20 μg/ml final). After overnight incubation and washing, sections were incubated for 2 h with anti-mouse HRP/Alexa Fluor-594 (4 μg/ml) (Invitrogen/Molecular Probes), washed again and placed onto slides for incubation with 3.3-

diaminobenzidine as a chromogen for HRP (BD Biosciences). Zink fixed tissues were deparaffinized and antigen retrieval performed in 1mM EDTA for 15 min at 100 °C followed by treatment as above. Tissues were incubated with primary antibodies anti-mouse F4/80 (5 μg/ml) (Cedarlane) or anti-human Ki67 (20 μg/ml) (BD Pharmingen) for 1h, followed by HRP-anti rat (4 μg/ml) (Jackson Immunoresearch) or biotinylated anti-mouse(7.5 μg/ml) (Vector Laboratories Inc.) antibodies respectively. Following the biotinylation step, tissues were treated with the vectastain ABC kit and all samples were subsequently treated with the peroxidase substrate Vector SG (Vector Laboratories Inc.). Slides were analyzed and images deconvoluted using an AxioImager M1m microscope and AxioVision 4.6 software (Zeiss, Thornwood, NY). Percent area covered by Ki67 or F4/80 signal relative to lesion area measured was measured with MetaMorph image processing software.

ScFv and ligand binding to purified αvβ3 receptor protein

Biotinylated natural ligands of αvβ3: vitronectin (VN), fibronectin (FN) or fibrinogen (Fg) (10μg/ml) were incubated with purified immobilized αvβ3 receptor protein in TBS containing Ca^{2+}, Mg^{2+}, and Mn^{2+} (1mM each), in the presence of increasing concentrations of purified scFv protein. A non-function blocking scFv directed against the integrin αv subunit, scFv 20, was used as a control. Ligand binding was measured after 1 h at 30°C using alkaline phosphatase-conjugated goat-anti-biotin antibody (Sigma at 1:200 dilution of serum), followed by a colorimetric substrate reaction.

Antibody cell binding kinetics

To define conditions for half maximal scFv binding, MDA-MB-$435_{\beta3D723R}$ cells were incubated with purified FLAG-tagged scFv protein in increasing concentrations of Mn^{2+} (3.75 μM-100 μM). Binding was measured by flow cytometry with murine M2 anti-FLAG antibody (15 μg/ml) (Sigma, St. Louis, MO) followed by FITC anti-mouse (30 μg/ml) (Pierce). Using the Mn^{2+} concentration (25 μM) that yielded half maximal scFv binding, scFv binding saturation was then measured by incubating MDA-MB-$435_{\beta3D723R}$ cells for 1h with increasing concentrations of directly FITC-labeled scFv 5 protein (2.34μg/ml-150μg/ml). The kinetics of scFv cell association and dissociation were analyzed by flow cytometry with directly FITC-labeled scFv protein at half maximal Mn^{2+} concentration and saturating scFv concentration, using MDA-MB-$435_{\beta3D723R}$ cells. Association time was measured after removing unbound ligand in 10 min intervals. To determine dissociation, cells were first allowed to bind scFv for 1 h to reach binding saturation, after which unbound ligand was removed and the cells washed, before measuring remaining bound scFv in 10 min intervals. FITC-labeled fibrinogen (Fg) was used as a natural ligand for comparison. All incubations were done on ice using ice-cold buffers to prevent scFv or ligand internalization.

Western blot analysis and Immunoprecipitation

To study scFv caspase-3 interaction, tumor cells were lysed in RIPA buffer and equal amounts of protein separated, blotted, and detected with rabbit-anti-caspase-3 antibody Sc7148 (0.5 μg/ml) (Santa Cruz) followed by goat-anti-rabbit-IgG/HRP conjugate (26.6 ng/ml) (Zymed, San Fransisco, CA). Caspase-3 was immunoprecipitated from cell lysates in the presence of protease inhibitors (Roche complete Mini tablet, EDTA-free and 2 mM PMSF) using goat-anti-caspase-3 antibody Sc1225 (1μg/100 μl lysate) (Santa Cruz) and

protein G sepharose beads. Control lysates were incubated with Protein G beads only. Precipitated proteins were analyzed on 4-20% SDS-PA gels, blotted and detected with rabbit-anti-caspase-3 (0.5 μg/ml) and goat-anti-rabbit-IgG/ HRP conjugate (26.6 ng/ml). Interaction between scFv antibodies and caspase-3 was analyzed by co-immuno precipitation using anti-caspase-3 as above. Flag-tagged scFv 5 (10 μg), or scFv Mut 5 (RGE mutant of scFv 5) as control, were added to cell lysates before western blotting with mouse-anti-Flag (1:500 of Sigma F3165), followed by donkey-anti-mouse-IgG (0.5 μg/ml). Controls included IP without scFv antibodies, addition of scFv 5 but no goat-anti-caspase-3 antibody, and a combination of beads, lysis buffer (instead of lysate) and either scFv 5 or scFv Mut 5.

ELISA-based analysis of caspase-3 and scFv interaction

To analyze binding of caspase-3 to the scFv antibodies, 96-well plates were coated with recombinant procaspase-3 (2 μg/ml) (BioVision, Moutain View, CA), blocked, and incubated with Flag tagged scFv 5 (1-15 μg/ml) or scFv Mut 5 (non RGD containing control) in the presence of 2mM $MnCl_2$. Binding was measured after incubation with mouse-anti-Flag (Sigma) and donkey-anti-mouse-IgG (Jackson Immuno Research Laboratories, West Grove, PA) (all antibodies used at 0.5 μg/ml).

Activation of caspase-3 in hypotonic cell lysates

Activation of caspase-3 in hypotonic lysates of 293A cells or as recombinant protein was measured at end points using the Caspase-Glo 3/7 Assay (Promega) and caspase-3/7 specific peptide sequence Asp-Glu-Val-Asp (DEVD). Hypotonic cell lysates were pepared as desribed (46). Cell lysates were combined with scFv 5 or scFvMut 5, or with RGD or RAD peptides. Cytochrome c/dATP was used as positive control and PBS as negative control. Samples were incubated for 1 h at 37°C, before adding Glo reagent (Promega, Madison, WI) and measuring bioluminescence as relative light units (RUL). GRGDNP was used as RGD peptide and GRADSP as RAD control as reported (27). Chromogenic substrate reactions were used for continuous measurements of caspase-3 activity. Hypotonic cell lysates were combined with scFv 5 or scFv Mut 5, and DEVD-pNA was added in excess to monitior absorption at 405 nm every 20 s for 2 h at 37°C. Cytochrome c/dATP was used as positive control. Maximum reaction velocity (V_{max}) was determined by graphing absorption versus time using the linear graph parts.

Activation of recombinant caspase-3

Recombinant procaspase-3 was expressed in *E. coli* and His-tag purified as described (47). Recombinant procaspase-3 was incubated with scFv 5, or scFv Mut 5 as control, in caspase assay buffer (50 mM HEPES, pH 7.5, 150 mM NaCl, 0.1% CHAPS, 10% sucrose, 10 mM DTT) in the presence of 1 mM Mg^{2+}. Granzyme B was used as a positive control. Activity was measured based on bioluminescence signal 30 min after adding Glo Reagent. For continuous measurement of recombinant caspase-3 activity, recombinant procaspase-3 was incubated with scFv 5, or scFv Mut 5 as negative control, in PBS with 10 mM DTT, with or without 4 mM $MgCl_2$ for 15 min at 37°C. Ac-DEVD-AFC (100 μM final) was added as fluorgenic caspase-3 substrate and fluorescence measured continuously for 30 min. V_{max} was determined by graphing fluorescence against time.

Acknowledgement

We thank Dr. J. Koziol of The Scripps Research Institute for statistical analyses

Grant support: NIH grants CA095458, CA112287 to BFH, CBCRP grants 12NB0176 and 13NB0180 to BFH and DOD grant W81XWH-08-1-0468 to BFH, and fellowships from the Swedish Research Council to KS, and from SG Komen to JSK and ML

References

1. Steeg PS. Heterogeneity of drug target expression among metastatic lesions: lessons from a breast cancer autopsy program. Clin Cancer Res. 2008; 14(12):3643–3645. [PubMed: 18559575]
2. Cooper CR, Chay CH, Pienta KJ. The Role of alpha(v)beta(3) in Prostate Cancer Progression. Neoplasia. 2002; 4(3):191–194. [PubMed: 11988838]
3. Brooks PC, Montgomery AM, Rosenfeld M, et al. Integrin alpha v beta 3 antagonists promote tumor regression by inducing apoptosis of angiogenic blood vessels. Cell. 1994; 79(7):1157–1164. [PubMed: 7528107]
4. Lim M, Guccione S, Haddix T, et al. alpha(v)beta(3) Integrin in central nervous system tumors. Hum Pathol. 2005; 36(6):665–669. [PubMed: 16021573]
5. Felding-Habermann B, O'Toole TE, Smith JW, et al. Integrin activation controls metastasis in human breast cancer. Proc Natl Acad Sci U S A. 2001; 98(4):1853–1858. [PubMed: 11172040]
6. Desgrosellier JS, Barnes LA, Shields DJ, et al. An integrin alpha(v)beta(3)-c-Src oncogenic unit promotes anchorage-independence and tumor progression. Nat Med. 2009
7. Albelda SM, Mette SA, Elder DE, et al. Integrin distribution in malignant melanoma: association of the beta 3 subunit with tumor progression. Cancer Res. 1990; 50(20):6757–6764. [PubMed: 2208139]
8. Gingras MC, Roussel E, Bruner JM, Branch CD, Moser RP. Comparison of cell adhesion molecule expression between glioblastoma multiforme and autologous normal brain tissue. J Neuroimmunol. 1995; 57(1-2):143–153. [PubMed: 7535788]
9. Gladson CL, Hancock S, Arnold MM, Faye-Petersen OM, Castleberry RP, Kelly DR. Stage-specific expression of integrin alphaVbeta3 in neuroblastic tumors. Am J Pathol. 1996; 148(5):1423–1434. [PubMed: 8623914]
10. Ding Q, Stewart J Jr. Olman MA, Klobe MR, Gladson CL. The pattern of enhancement of Src kinase activity on platelet-derived growth factor stimulation of glioblastoma cells is affected by the integrin engaged. J Biol Chem. 2003; 278(41):39882–39891. [PubMed: 12881526]
11. Brooks PC, Clark RA, Cheresh DA. Requirement of vascular integrin alpha v beta 3 for angiogenesis. Science. 1994; 264(5158):569–571. [PubMed: 7512751]
12. Fujita Y, Abe R, Shimizu H. Clinical approaches toward tumor angiogenesis: past, present and future. Curr Pharm Des. 2008; 14(36):3820–3834. [PubMed: 19128235]
13. Cai W, Chen X. Anti-angiogenic cancer therapy based on integrin alphavbeta3 antagonism. Anticancer Agents Med Chem. 2006; 6(5):407–428. [PubMed: 17017851]
14. Desgrosellier JS, Cheresh DA. Integrins in cancer: biological implications and therapeutic opportunities. Nat Rev Cancer. 2010; 10(1):9–22. [PubMed: 20029421]
15. Paolillo M, Russo MA, Serra M, Colombo L, Schinelli S. Small molecule integrin antagonists in cancer therapy. Mini Rev Med Chem. 2009; 9(12):1439–1446. [PubMed: 19929817]
16. Schottelius M, Laufer B, Kessler H, Wester HJ. Ligands for mapping alphavbeta3-integrin expression in vivo. Acc Chem Res. 2009; 42(7):969–980. [PubMed: 19489579]
17. Felding-Habermann B, Lerner RA, Lillo A, et al. Combinatorial antibody libraries from cancer patients yield ligand-mimetic Arg-Gly-Asp-containing immunoglobulins that inhibit breast cancer metastasis. Proc Natl Acad Sci U S A. 2004; 101(49):17210–17215. [PubMed: 15563590]
18. Carter PJ. Potent antibody therapeutics by design. Nat Rev Immunol. 2006; 6(5):343–357. [PubMed: 16622479]
19. Chambers AF. MDA-MB-435 and M14 Cell Lines: Identical but not M14 Melanoma? Cancer Res. 2009; 96(13):5292–5293. [PubMed: 19549886]

20. Hollestelle A, Schutte M. Comment Re: MDA-MB-435 and M14 cell lines: identical but not M14 Melanoma? Cancer Res. 2009; 69(19):7893. [PubMed: 19723654]
21. Deryugina EI, Quigley JP. Chick embryo chorioallantoic membrane model systems to study and visualize human tumor cell metastasis. Histochem Cell Biol. 2008; 130(6):1119–1130. [PubMed: 19005674]
22. Byzova TV, Kim W, Midura RJ, Plow EF. Activation of integrin alpha(V)beta(3) regulates cell adhesion and migration to bone sialoprotein. Exp Cell Res. 2000; 254(2):299–308. [PubMed: 10640428]
23. Luo BH, Carman CV, Springer TA. Structural Basis of Integrin Regulation and Signaling. Annu Rev Immunol. 2007; 25:619–647. [PubMed: 17201681]
24. Ajroud K, Sugimori T, Goldmann WH, Fathallah DM, Xiong JP, Arnaout MA. Binding Affinity of Metal Ions to the CD11b A-domain Is Regulated by Integrin Activation and Ligands. J Biol Chem. 2004; 279(24):25483–25488. [PubMed: 15070893]
25. Xiong JP, Stehle T, Goodman SL, Arnaout MA. Integrins, cations and ligands: making the connection. J Thromb Haemost. 2003; 1(7):1642–1654. [PubMed: 12871301]
26. Xiong JP, Stehle T, Goodman SL, Arnaout MA. New insights into the structural basis of integrin activation. Blood. 2003; 102(4):1155–1159. [PubMed: 12714499]
27. Buckley CD, Pilling D, Henriquez NV, et al. RGD peptides induce apoptosis by direct caspase-3 activation [see comments]. Nature. 1999; 397(6719):534–539. [PubMed: 10028971]
28. Roy S, Bayly CI, Gareau Y, et al. Maintenance of caspase-3 proenzyme dormancy by an intrinsic “safety catch” regulatory tripeptide. Proc Natl Acad Sci U S A. 2001; 98(11):6132–6137. [PubMed: 11353841]
29. Anuradha CD, Kanno S, Hirano S. RGD peptide-induced apoptosis in human leukemia HL-60 cells requires caspase-3 activation. Cell Biol Toxicol. 2000; 16(5):275–283. [PubMed: 11201051]
30. Aguzzi MS, Giampietri C, De Marchis F, et al. RGDS peptide induces caspase 8 and caspase 9 activation in human endothelial cells. Blood. 2004; 103(11):4180–4187. [PubMed: 14982875]
31. Janicke RU, Ng P, Sprengart ML, Porter AG. Caspase-3 is required for alpha-fodrin cleavage but dispensable for cleavage of other death substrates in apoptosis. J Biol Chem. 1998; 273(25): 15540–15545. [PubMed: 9624143]
32. Devarajan E, Sahin AA, Chen JS, et al. Down-regulation of caspase 3 in breast cancer: a possible mechanism for chemoresistance. Oncogene. 2002; 21(57):8843–8851. [PubMed: 12483536]
33. Byzova TV, Rabbani R, D'Souza SE, Plow EF. Role of integrin alpha(v)beta3 in vascular biology. Thromb Haemost. 1998; 80(5):726–734. [PubMed: 9843163]
34. Stupack DG, Cheresh DA. Integrins and angiogenesis. Curr Top Dev Biol. 2004; 64:207–38. [PubMed: 15563949]
35. McNeel DG, Eickhoff J, Lee FT, et al. Phase I trial of a monoclonal antibody specific for alphavbeta3 integrin (MEDI-522) in patients with advanced malignancies, including an assessment of effect on tumor perfusion. Clin Cancer Res. 2005; 11(21):7851–7860. [PubMed: 16278408]
36. Stupack DG, Cheresh DA. Get a ligand, get a life: integrins, signaling and cell survival. J Cell Sci. 2002; 115(Pt;%19):3729–3738. [PubMed: 12235283]
37. Takagi J, Springer TA. Integrin activation and structural rearrangement. Immunol Rev. 2002; 186:141–163. [PubMed: 12234369]
38. Holliger P, Hudson PJ. Engineered antibody fragments and the rise of single domains. Nat Biotechnol. 2005; 23(9):1126–1136. [PubMed: 16151406]
39. Colcher D, Pavlinkova G, Beresford G, Booth BJ, Choudhury A, Batra SK. Pharmacokinetics and biodistribution of genetically-engineered antibodies. Q J Nucl Med. 1998; 42(4):225–241. [PubMed: 9973838]
40. Mao S, Gao C, Lo CH, Wirsching P, Wong CH, Janda KD. Phage-display library selection of high-affinity human single-chain antibodies to tumor-associated carbohydrate antigens sialyl Lewisx and Lewisx. Proc Natl Acad Sci U S A. 1999; 96(12):6953–6958. [PubMed: 10359820]
41. Krag DN, Fuller SP, Oligino L, et al. Phage-displayed random peptide libraries in mice: toxicity after serial panning. Cancer Chemother Pharmacol. 2002; 50(4):325–332. [PubMed: 12357308]

42. Jaffe CC. Measures of response: RECIST, WHO, and new alternatives. J Clin Oncol. 2006; 24(20): 3245–3251. [PubMed: 16829648]
43. Therasse P, Eisenhauer EA, Verweij J. RECIST revisited: a review of validation studies on tumour assessment. Eur J Cancer. 2006; 42(8):1031–1039. [PubMed: 16616487]
44. Eisenhauer EA, Therasse P, Bogaerts J, et al. New response evaluation criteria in solid tumours: revised RECIST guideline (version 1.1). Eur J Cancer. 2009; 45(2):228–247. [PubMed: 19097774]
45. Agresti A. Categorical Data Analysis. Sec. 3.3.7. ed. 1990
46. Denault JB, Salvesen GS. Expression, purification, and characterization of caspases. Curr Protoc Protein Sci. 2003 Chapter 21:Unit 21.13.: Unit.
47. Stennicke HR, Jurgensmeier JM, Shin H, et al. Pro-caspase-3 is a major physiologic target of caspase-8. J Biol Chem. 1998; 273(42):27084–27090. [PubMed: 9765224]

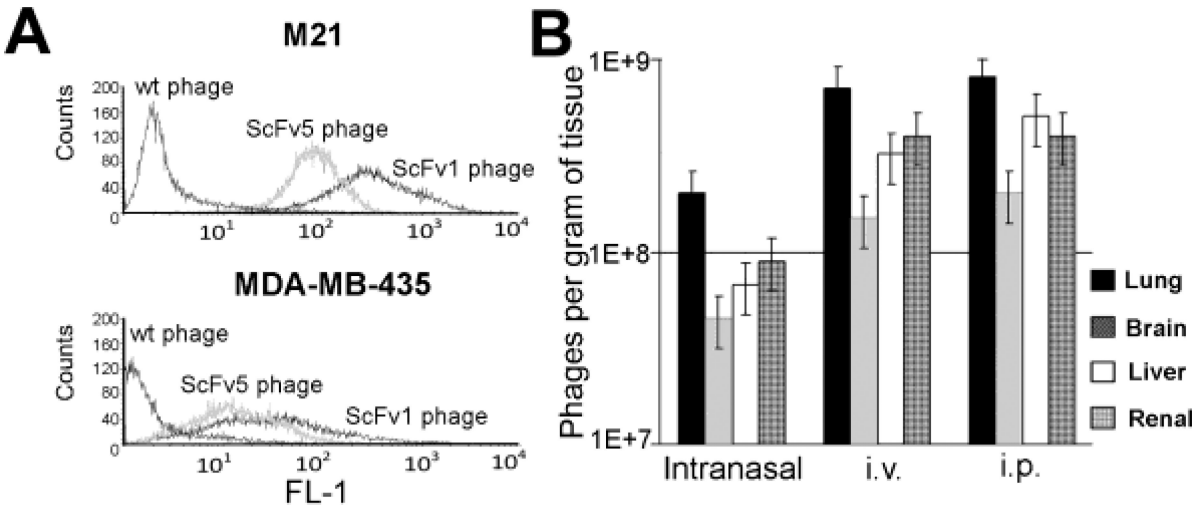

Figure 1. Antibody binding validation and routes of administration

(A) Before use in animals, the binding properties of each scFv phage batch were analyzed by flow cytometry on tumor cells expressing high affinity integrin αvβ3. scFv phage was tested in the presence of calcium on M21 human melanoma cells that carry activated αvβ3 and on MDA-MB 435 cells which express mutant $\alpha v\beta 3_{D723R}$. **(B)** scFv phage organ distribution in the mouse model. Phage were injected i.v., i.p. or applied intranasally to non-tumor bearing mice to determine phage organ distribution 24 h later.

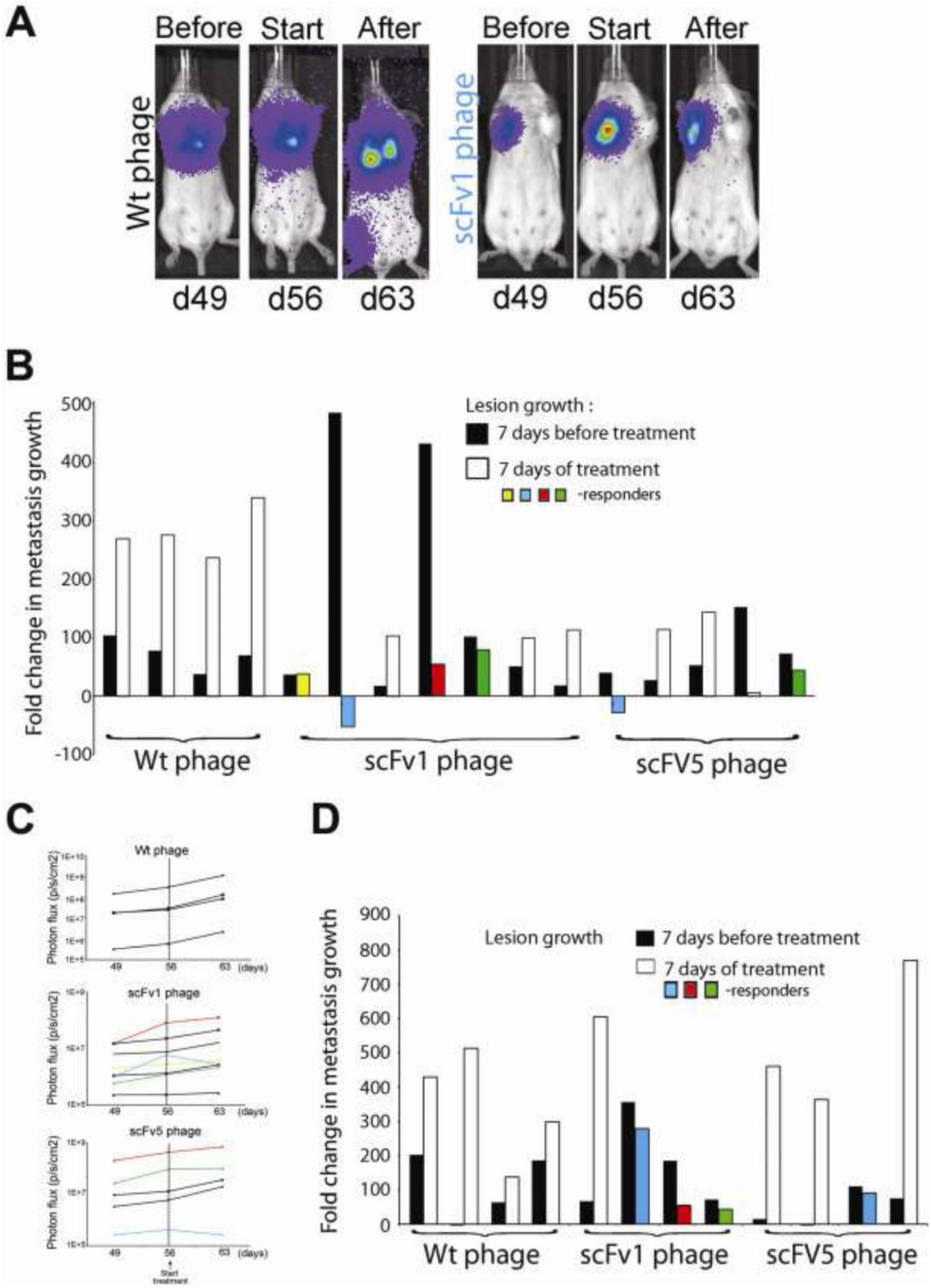

Figure 2. Lung metastases regress in response to treatment with scFv 1 or scFv 5

F-luc tagged MDA-MB-435 cells were injected i.v. and lesion development monitored by non-invasive bioluminescence imaging (photons/second/cm^2) over time. Treatment with scFv phage (5×10^{10} per dose) started on day 56 post tumor cell injection. **(A)** Examples of non- invasive bioluminescence imaging of representative animals that had received 1×10^5 tumor cells before treatment on day 49, at treatment onset on day 56, and after 4 doses of treatment on day 63. Reduced progression in lung lesions is seen after treatment with scFv1 but not with Wt-phage. **(B)** Response to treatment given every 48 h (4 doses). Fold-changes

of lesion growth were calculated based on growth during 7 days before treatment compared to 7 days under treatment. ScFv1-phage treatment yielded a 57% animal response rate in lung burden and one animal with stabilization of lesion growth. ScFv5-phage treatment resulted in a 60% animal response rate for lung burden. Wt-phage gave no reduction in tumor growth. **(C)** *Non*-invasive bioluminescence imaging of lung burden (photons/second/cm^2) over time before and during treatment. Animals were treated every 48h for (4 doses). Lung lesion growth was monitored pre-treatment (day 49-56) and during treatment until day 63 (the end of treatment). Dashed vertical lines indicate the start of treatment on day 56. Animals responding to treatment are colored. **(D)** Response of mice with very advanced metastatic burden, induced by injecting 2.5×10^5 tumor cells, to treatment given every 24h (8 doses). Treatment with Wt-phage gave no response, whereas regression and reduced tumor progression was seen in the scFv treated animals. ScFv1-phage treatment yielded a response in 75% of the animals, and scFv5-phage in 25%. Animals responding to treatment are colored.

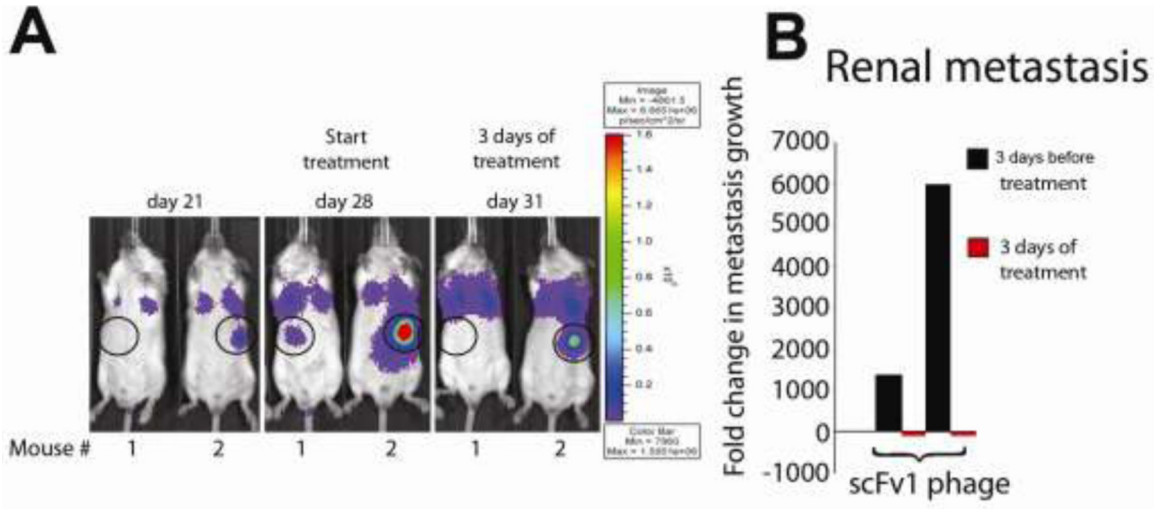

Figure 3. Examples of extrapulmonary lesion regression under treatment with scFv 1

(A) *F-luc* tagged, *in vivo* selected and highly metastatic MDA-MB-435-met cells were injected i.v. to induce multiorgan metastasis. Metastatic progression was monitored by non-invasive bioluminescence imaging (photons/second/cm^2) over time. In these examples, the location of renal lesions is circled and shown 3 days before treatment, at the beginning of treatment, and after 3 daily doses of scFv1 phage. **(B)** Fold-change in renal lesion growth, calculated based on signal change during 3 days before and 3 days under treatment.

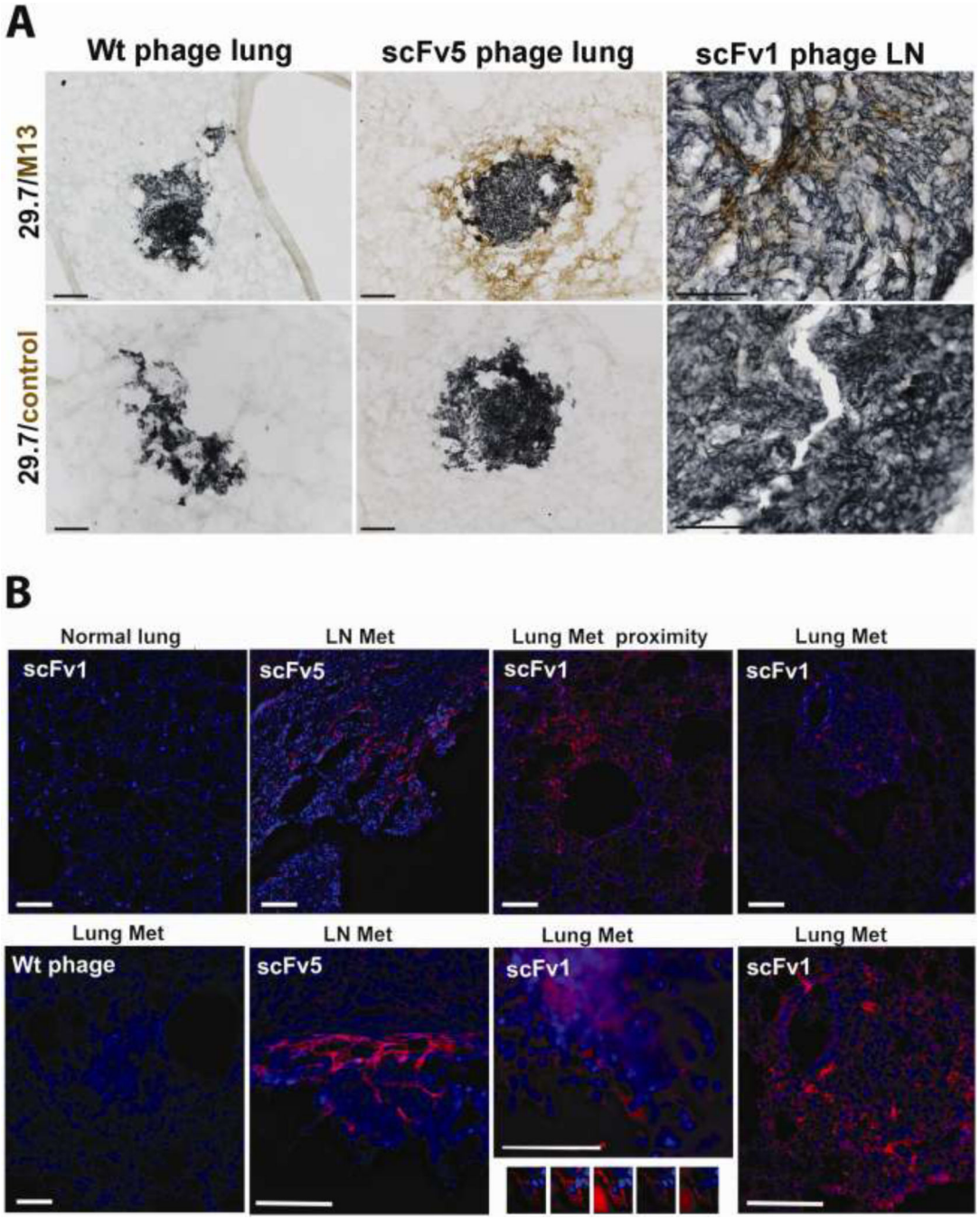

Figure 4. Localization of scFv1 or scFv 5 phage to areas in and around metastatic lesions in mice with multi-organ metastasis

(A) Immunohistochemical detection of phage homing to metastases in the lungs and lymph node. ScFv phage, or wt control phage, were injected i.p. daily for 7 days into tumor bearing mice. 24h after the last scFv dose, the animals were terminally perfused and frozen tissue sections stained with mAb 29.7 (dark blue), specific for human CD44 indicating the tumor cells, and anti-M13 mAb to detect phage (DAB, brown). Animals treated with wt-phage did not show phage localization to tumor metastases (left panels), but lung metastasis from scFv5-phage treated animals showed phage localization in the tumor proximity as well as

within the lung lesion (middle). A lymph node metastasis from an animal treated with scFv1-phage showed phage localizing to the tumor bulk as well as to the outer border of the lesion (right). Controls treated with secondary antibody and substrate did not show specific staining in or around any lesions. Scale bars indicate 100μm. **(B)** Fluorescence microscopy detecting phage (red). (Upper row) M13 phage was detected in and around lung metastases of scFv1-phage treated animals (right), as well as within the near proximity of the tumor lesions (second right), with minimal phage signal in the unaffected lung tissue away from a tumor lesion (left). Lymph node metastasis showed scFv1-phage localization in the tumor mass and within the tumor proximity (second left, top and bottom). Animals treated with wt-phage showed no specific staining in tumor lesions. Only a weak signal was sometimes seen in non-tumor bearing parts of the tissues, comparable to that seen for scFv phage in unaffected areas of lung tissue (lower left). Using optical sectioning and deconvolution of *z*-stack images, scFv phage was specifically detected associated with tumor cells (lower second right). Scale bars indicate 100 μm.

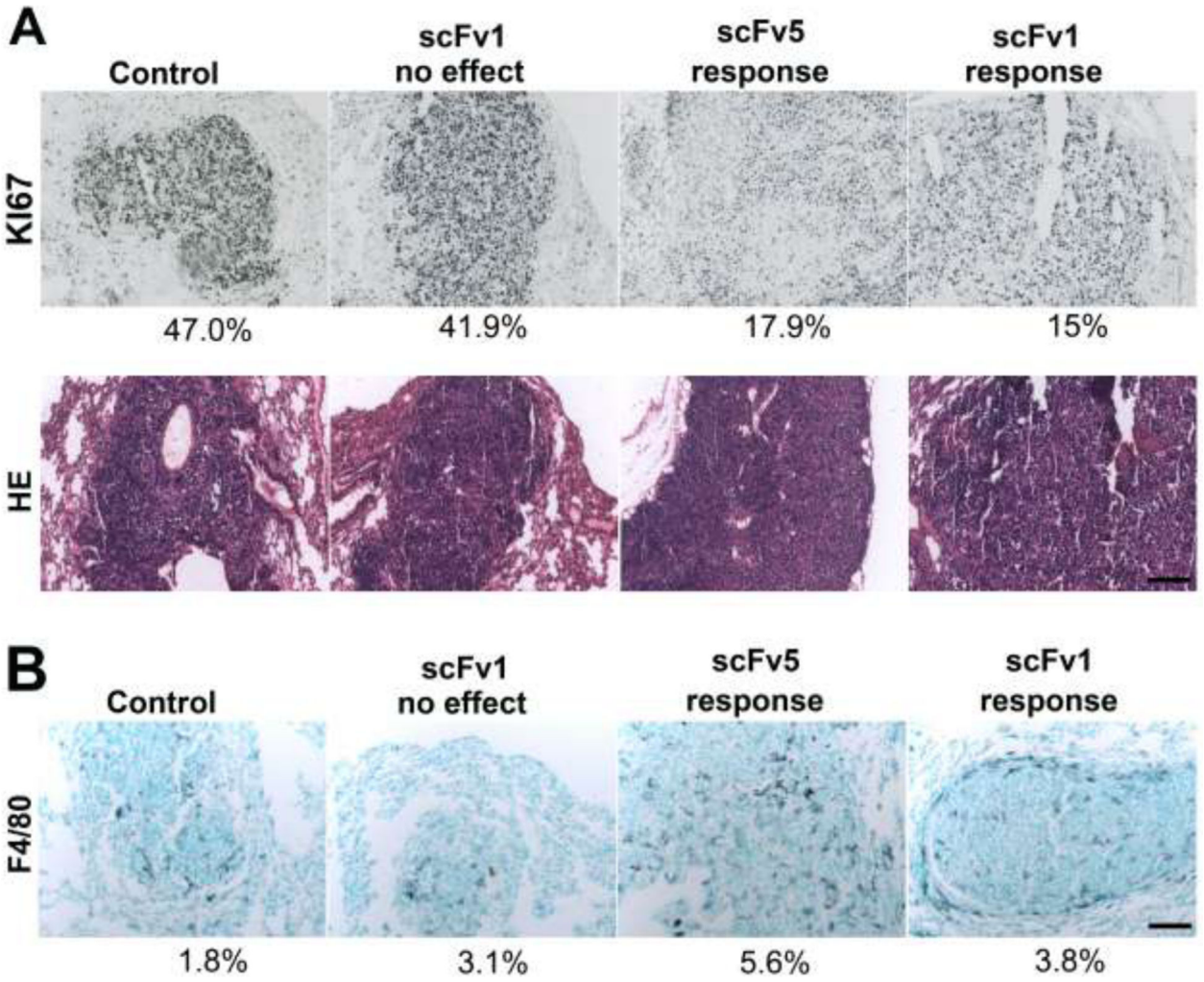

Figure 5. Effects of scFv treatment on tumor cells in vivo and host cell infiltration

(A) Ki67 staining of lung metastases treated with wt-phage or scFv1/5-phage (top panel). Lesions in animals responding to treatment showed fewer proliferating cells. Percent area covered by Ki67 signal relative to lesion area measured. H&E staining of the lesions (lower panel). **(B)** F4/80 macrophage staining of lung metastases in mice treated with wt-phage or scFv1/5-phage. An increased infiltrate was seen in lesions responding to treatment. Percent area covered by F4/80 signal relative to lesion area measured. Scale bars indicate 100 μm in all sections.

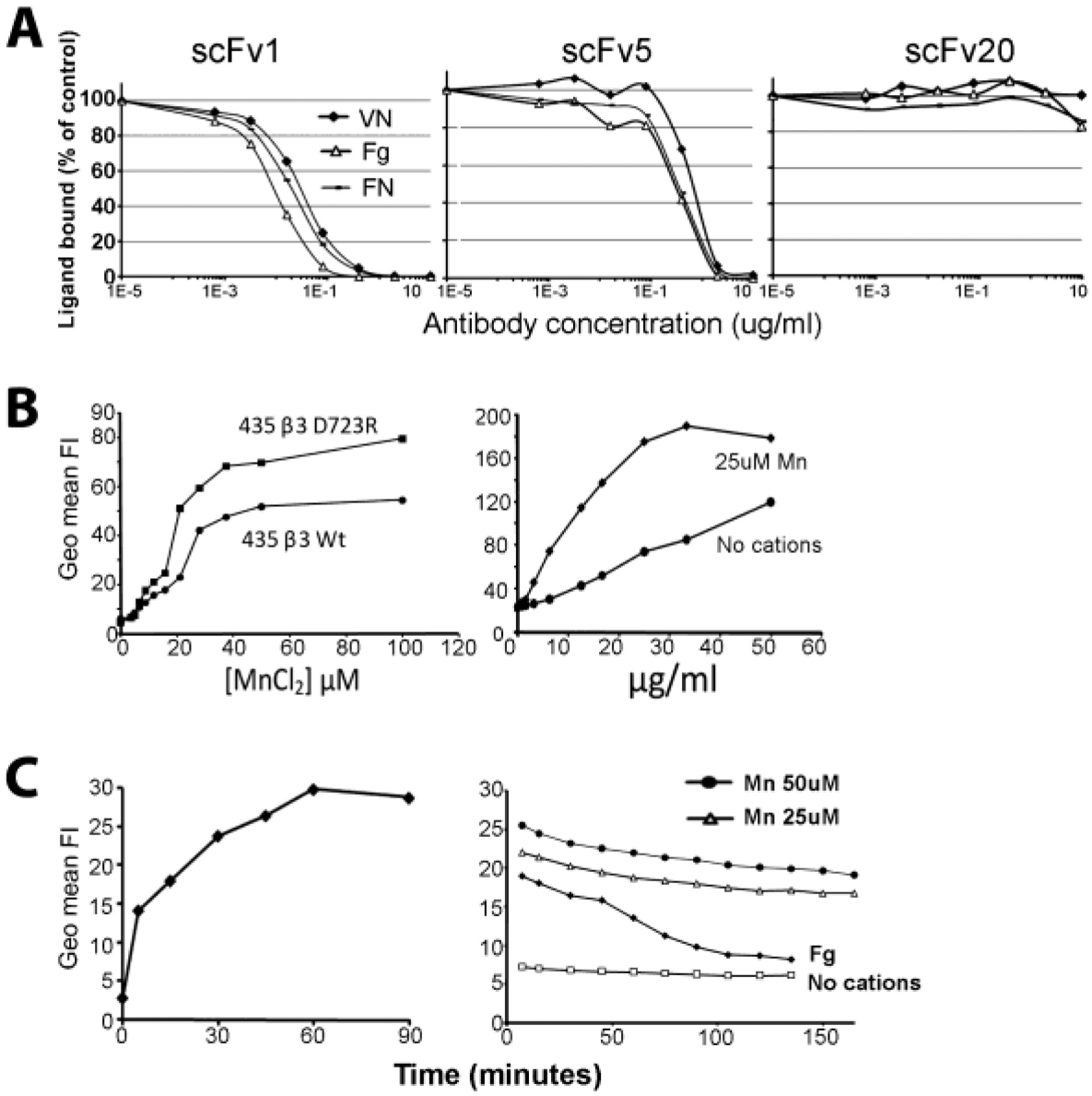

Figure 6. Inhibitory and binding properties of scFv 1 and scFv5

(A) Biotinylated natural ligands of αvβ3: vitronectin (VN), fibronectin (FN) or fibrinogen (Fg) (10μg/ml) were incubated with purified immobilized αvβ3 receptor protein in TBS containing Ca^{2+}, Mg^{2+}, and Mn^{2+} (1mM each), in the presence of increasing concentrations of purified scFv protein. A non-function blocking scFv directed against the integrin v subunit, scFv 20, was used as a control. **(B)** Flow cytometric binding analysis of fluorescinated scFv5 protein and MDA-MB 435 human tumor cells, expressing either activated high-affinity $\alpha v\beta 3_{D723R}$ or non-activated $\alpha v\beta 3_{WT}$. Binding was experimentally maximized in the presence of Mn^{2+}, known to induce a high affinity state in integrin heterodimers. Using a Mn^{2+} concentration (25 μM) that supports suboptimal scFv5 binding to tumor cells expressing activated $\alpha v\beta 3_{D723R}$, antibody was titrated to determine binding saturation. **(C)** Kinetics of scFv cell association and dissociation were analyzed by flow cytometry with FITC-labeled scFv protein at half maximal Mn^{2+} concentration and

saturating scFv concentration, using MDA-MB-435$_{\beta 3D723R}$ cells. (Left) Association time was measured after removing unbound ligand in 10 min intervals. (Right) Dissociation was determined after allowing cells to bind scFv for 1 h to reach binding saturation, followed by removal of unbound ligand, washing and measuring scFv that remained bound in 10 min intervals. FITC-labeled fibrinogen (Fg) was used as a natural ligand for comparison. All incubations were done on ice using ice-cold buffers to prevent scFv or ligand internalization. No binding was detected in the absence of divalent cations.

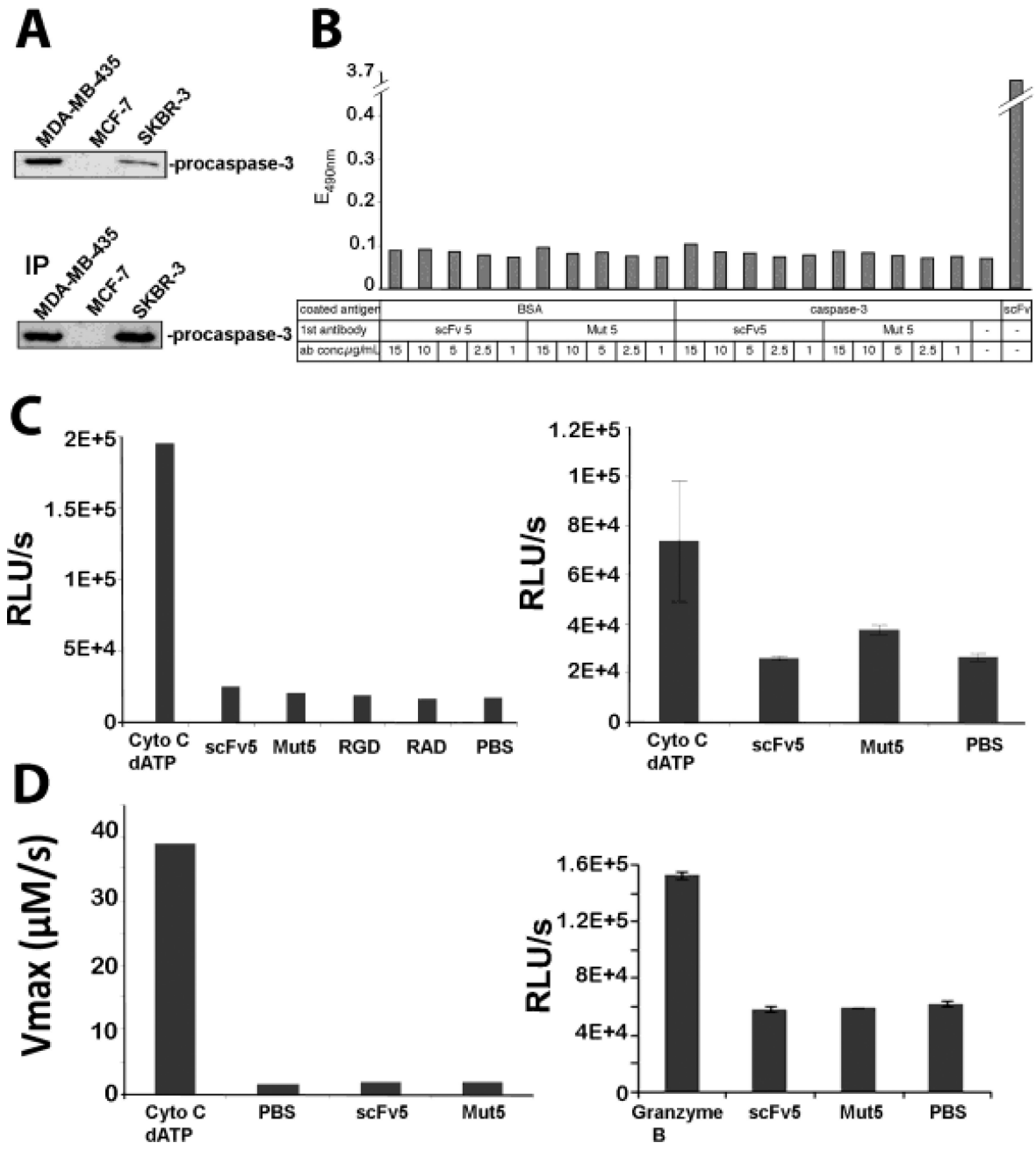

Figure 7. Caspase-3 expression in the target tumor cells and analysis of caspase-3 binding and activation by RGD-containing scFv1 and scFv5

(A) (Top) Western blot analysis of caspase-3 expression in MDA-MB-435, MCF-7 (negative control) and SKBR-3 (positive control) cells. (Bottom) Verification for procaspase-3 by immunoprecipitation of caspase-3 from tumor cell lysates. **(B)** ELISA-based analysis of caspase-3 and scFv antibody interaction. Plates were coated with recombinant pro-caspase-3 or BSA (negative control) or scFv 5 (positive control). Addition of RGD-containing scFv 5 or RGE-containing scFv Mut 5 antibody, at concentrations as indicated showed no specific binding to caspase-3. **(C)** Analysis of caspase-3 activation by scFv antibodies. Hypotonic cell lysates, depleted of mitochondria, were combined with either scFv 5 or scFvMut 5 (4

μM), or RGD or RAD peptides (1 mM) (left panel). Cytochrome c/dATP were used as positive control and PBS as negative control in a bioluminescence assay. Cytochrome c and dATP were able to activate caspase-3 in the lysates, whereas all other samples showed only background signal. A higher scFv concentration was used to verify the lack of activation (10 μM) in the presence of Mg^{2+} (right panel). **(D)** Continuous measurement of caspase-3 activity in cell lysates based on chromogenic substrate reaction. Cleavage of colorimetric capsase 3 substrate N-acetyl-Asp-Glu-Val-Asp-*p*-nitroanilide (Ac-DEVD-*p*NA) was measured after combining hypotonic cell lysates with either scFv 5 or scFvMut 5 (2 μM). Absorption was measured continuously for 2 h at 37°C (left panel). Activation measurement of recombinant caspase-3 by scFv 5 or scFvMut 5 in the presence of Mg^{2+} using Granzyme B as positive and PBS as negative control. After 30 min incubation at 37°C, Glo reagent was added and bioluminescence measured after 30 min incubation at RT (right panel).

Table 1

Overview of treatment responsiveness in animals with advanced metastatic burden and response types

Response categories:	
Fold-changes in overall lesion growth, p/sec/cm^2, comparing same time span before and under treatment	
Progression:	≥ 1.3 fold
Stabilization:	0.7 fold - 1.3 fold
Reduced progression:	0.1 fold - 0.7 fold
Regression:	≤ 0.1 fold

Response category	**ScFv1**	**ScFv5**	**Control**
Progression	7/19	9/15	15/16
Stabilization	4/19	1/15	1/16
Reduced Progression	4/19	3/15	0/16
Regression	4/19	2/15	0/16

Compared to controls, treatment response was seen in a significant number of animals receiving scFv1 or scFv5 ($p= 0.0164$, Fisher exact test). There was no significant difference between responses to scFv1 compared to scFv5 ($p=0.55$, Fisher's exact test).

For comparison of responses between the three groups, scFv1, scFv5, and controls, we note that the overall likelihood ratio chi-squared statistic with 6 degrees of freedom may be partitioned into two independent components, each with 3 degrees of freedom: the first component corresponds to comparison of scFv1 vs scFv5, and the second component corresponds to the comparison of controls to the pooled scFv1/scFv5 category (45).

Table 2

Overview of regresssion in multiorgan metastasis

Regression	ScFv 1	ScFv 5	Control
Pulmonary lesions	3/9	2/6	0/7
Extrapulmonary lesions	4/9	0/6	0/7

Regression of metastatic burden was based on comparing lesion growth during the same time before versus under treatment, measured by bioluminescence imaging and fold-changes in photon flux (p/sec/cm^2) as in Table 1. Due to the heterogeneity of lesion burden and organ involvement, only regression responses are shown, and pulmonary versus extrapulmonary lesions are listed separately. Considering responses of lesions at all sites, scFv1 - but not scFv5 - lead to regression of multi-organ metastasis in a significant number of animals (7/9 scFv1, 2/6 scFv5, 0/7 control; p=0.0073 Fisher's exact test).